Quantum Network Coding on a Superconducting Processor

H Rall, M S Tame

Department of Physics, Stellenbosch University, Private Bag X1, Matieland, South Africa

E-mail: hjalmar.rall1@gmail.com

Abstract. An important consideration for quantum communication within the current noisy intermediate-scale quantum regime is the resource requirements of routing information within a complex network such as a quantum internet. Quantum network coding (QNC) reduces the resource requirements for simultaneous communication over a network by eliminating the problem of contention for network resources. In this work we implement measurement-based QNC (MQNC) on the latest generation IBM Q superconducting processor `ibm_cairo` by making use of an alternative to SWAP-based transpiling and demonstrate that improvements in processor hardware allow for greatly improved fidelity of the protocol compared to a prior work. Using these improved results we study noise within the code and identify a major contributor to noise in the final states.

1. Introduction

A major goal in the development of quantum computers and quantum communication is the creation of a quantum internet [1] which would allow the establishment of entanglement between multiple pairs of distant end nodes using a single common quantum communication network. By making use of a shared network, the resource cost of performing tasks such as quantum key distribution (QKD) and distributed quantum computing is greatly reduced compared to the scenario where each pair of end nodes must share a direct quantum communication channel. This holds also for the case of communication within a single processor.

Simple quantum networks are starting to become feasible with, for example, a 3-qubit solid state network [2] and a large scale QKD network with a satellite link [3] being demonstrated successfully. Furthermore, there is ongoing research into enabling optical communication between superconducting quantum processors [4, 5], which raises the possibility of using quantum processors to control more complex quantum networks in the near future. Thus the hardware for a quantum internet may be developed in the near future, but this hardware will still fall under the noisy intermediate scale quantum (NISQ) regime where the number of qubits is limited and gates increase the amount of noise in the system. Accordingly steps must be taken to make efficient use of the available resources.

The major disadvantage of a shared network (whether classical or quantum) is that routing information along a path between end nodes means that channels along the path become unavailable for other messages if the channels do not have sufficient capacity. If such a clash between routes exists and no alternate routing is available, the situation is referred to as contention. If routing is to be used, the only resolution to this problem is time-multiplexing, where some of the

messages are delayed while the others are sent. This has the effect of reducing the bandwidth (information transfer per unit time) of the channel. This problem can be circumvented by making use of network coding, or the analogous quantum network coding (QNC) [6, 7] instead of routing.

Measurement-based quantum network coding (MQNC) [8] is a variation on QNC which offers greater simplicity and reduced gate count by making use of measurement-based computing. MQNC was recently performed on a previous-generation IBM superconducting processor by Pathumsoot et al. [9], but processor noise proved too high to obtain useful final states. By making use of a novel transpiling technique we implemented MQNC on newer IBM hardware and show that the improvements in the hardware allow for greatly improved quality of the final states. We also investigate the role of depolarising noise in gates on the quality of the final state, and discuss the implications of our results.

2. Background

2.1. Graph States

MQNC falls within the category of measurement-based quantum algorithms. These make use of entangled states known as graph states which have the property that their qubits and entanglement correspond directly to the edges and vertices of an undirected graph. A graph $G(V, E)$ with vertex set V and edge set E defines a graph state with a statevector given by

$$|G\rangle = \prod_{i \neq j; i,j \in G} CZ_{i,j}^{\Gamma_{i,j}} \bigotimes_{k=1}^{n} |+\rangle_k \,,$$

where $\Gamma_{i,j}$ is the adjacency matrix of the underlying graph. There are a number of local operations and measurements which serve to transform one graph state into another [10], the two most useful of which are summarised below :

- **T1:** A Z-basis measurement on a qubit a removes the corresponding vertex and incident edges from the graph.
- **T2:** X-basis measurements on two adjacent qubits a and b removes them and complements the bipartite subgraph induced by N_a and N_b. i.e. $G(V, E) \rightarrow G(V/\{a, b\}, E\Delta K)$ with K the complete bipartite subgraph induced by $N_a \cup \{a\}$ and $N_b \cup \{b\}$. In other words, all the neighbours of a are connected to all the neighbours of b unless a connection already exists, in which case it is broken.

2.2. Network Coding

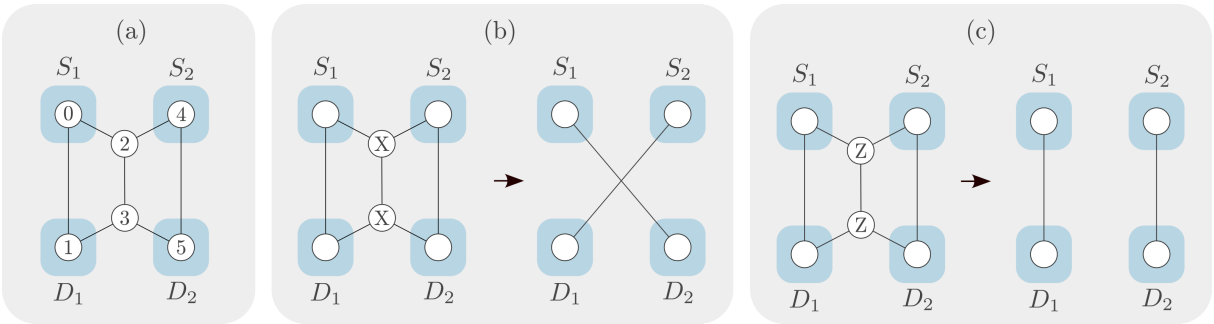

Figure 1. (a) The 6-qubit resource state for MQNC. (b) Creation of cross pairs via X-measurements. (c) Creation of straight pairs via Z-measurements. White circles represent qubits and lines represent entanglement, corresponding to the vertices and edges of a graph respectively. Blue squares represent end nodes in the network.

MQNC solves contention in the butterfly network, shown in Fig. 1 (a). The goal is to be able to manipulate the network to achieve either of the two final states shown on the right hand sides of Fig. 1 (b) and (c). This is achieved by performing either two X-measurements (Rule T2) or two Z-measurements (Rule T1) on the central qubits as shown. The final 2-qubit graph states can subsequently be used for communicating quantum information by means of teleportation. By using measurements to redistribute the existing entanglement (communication channels) the network has been reconfigured so that the bottleneck no longer exists.

3. Experimental implementation

The current generation of IBM Q processors have the layout shown in Fig. 2. Unlike the prior experiment in Ref. [9] which made use of the grid-like layout of the older IBM Q 20 Tokyo processor, it is not possible to directly create the 6-qubit resource state necessary for MQNC on this new layout. It is possible to transpile quantum circuits to layouts on which they cannot be executed directly, but this ordinarily requires the use of noisy SWAP operations to move logical qubits to adjacent physical qubits before they can be entangled. In the case of graph states however there is an alternative. By making use of local complementation (LC) [10] it is possible to redistribute entanglement in a controlled manner using only single-qubit operations. Using LC, we were able to create the MQNC resource state on `ibm_cairo` using only seven 2-qubit gates as opposed to the much larger number required for SWAP-based transpiling.

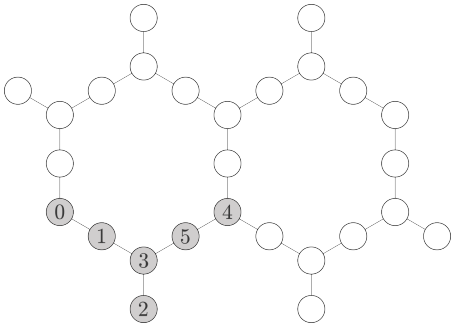

Figure 2. Layout of `ibm_cairo`. Edges indicate neighbouring qubits on which CNOT gates may be performed. Light grey qubits are used to create the 6-qubit resource state for the network code.

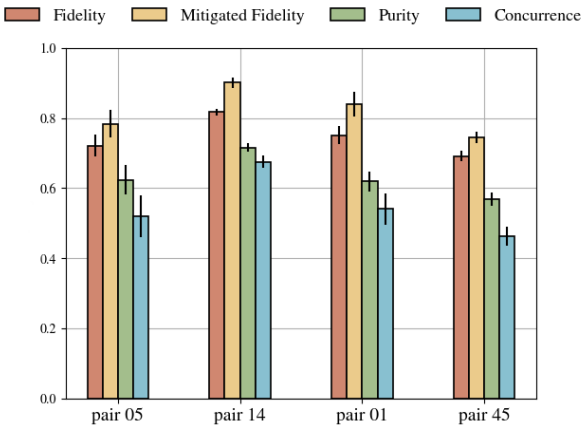

Figure 3. Results of full state tomography on the 2-qubit entangled states generated using the MQNC protocol on `ibm_cairo`. Fidelity is shown before and after application of readout error mitigation on the 2 qubits.

I performed MQNC as outlined in Fig. 1 on the IBM Q falcon superconducting processor `ibm_cairo` using LC instead of standard transpiling. This is a 27-qubit device with the layout shown in Fig. 2. The processor was accessed remotely through the IBMQ API and the QISKIT Python library.

A single run of the experiment constitutes calibration for readout error mitigation and state tomography of one of the two qubit graph states (pairs) generated using MQNC. This is repeated for each of the four pairs in turn, and the whole procedure is then repeated 30 times to account for variation in processor noise. The runs were spread out between 9PM 26 Apr 2022 and 5AM 27 Apr 2022 (UTC) due to use of the fair-share queuing system. The variation in processor noise is found to be sufficiently small over a time-scale of minutes that the delay between calibration and experiment is not significant and results are not skewed by varying noise from one pair to

the next. The measurements in the protocol result in probabilistic byproduct operations on the desired final state. The IBM processors do not support the feed-forward functionality necessary to undo these operations, so results must be post-selected based on measurement outcomes. The four possible outcomes of two measurements at the central qubits of the network code correspond to four possible byproducts (including the identity) on each of the final 2-qubit states, which occur with equal probability so that 1/4 of the results are kept.

In order to measure the quality of the state generated and to compare to the results of the previous study [9], I perform quantum state tomography [11] on each of the four pairs that can be generated using MQNC. Readout error mitigation is then applied to the results, and they are subsequently post-selected so as to correspond to the byproduct-free graph state. 4000 shots are used for each of the 9 tomography circuits so that approximately 1000 shots remain after post-selection. Density matrices are obtained from the tomography results, and the fidelity compared to the ideal state $|G_2\rangle = \frac{1}{\sqrt{2}}(|0+\rangle + |1-\rangle)$, as well as the purity and concurrence are calculated. The results are shown in Fig. 3 and are compared to those of the prior experiment in Table 1. Note that only values for the cross pairs are reported in Ref. [9]. As in the prior experiment, the fidelity is defined as

$$F(\rho_1, \rho_2) = \left(\mathrm{Tr}\sqrt{\sqrt{\rho_1}\rho_2\sqrt{\rho_1}}\right)^2.$$

Fidelity is a measure of the overlap between quantum states, having a value of 1 for identical states and 0 for orthogonal states. In addition to fidelity, we also consider the concurrence, an entanglement monotone defined according to

$$C(\rho) = \max\{0, \lambda_1 - \lambda_2 - \lambda_3 - \lambda_4\},$$

where the λ_i are the square roots of the eigenvalues of $\tau = \rho(Y \otimes Y)\rho^*(Y \otimes Y)$ in descending order.

Despite the additional noise incurred by the transpiling process, `ibm_cairo` shows a significant improvement in both fidelity and concurrence over the results of Pathumsoot et al. [9]. Notably, the improvement in concurrence proves that a higher degree of entanglement has been established in the final state.

Table 1. Comparison of the new results on `ibm_cairo` with the prior experiment by Pathumsoot et al. on IBM Q 20 Tokyo.

	New Results	Pathumsoot et al. [9]
Fidelity cross pair 1	0.75 ± 0.05	0.57 ± 0.01
Fidelity cross pair 2	0.83 ± 0.03	0.58 ± 0.01
Concurrence cross pair 1	0.5 ± 0.10	0.25 ± 0.02
Concurrence cross pair 2	0.61 ± 0.06	0.36 ± 0.02

4. Noise Modelling

While the results presented above demonstrate that recent improvements in superconducting processor technology have significantly improved the fidelity with which MQNC can be performed, the final states are still significantly affected by processor noise. It is therefore of interest to study how noise affects the protocol.

The three main sources of error in the IBMQ processors are gate infidelities, state-preparation and measurement errors, and thermal decoherence and dephasing [12]. All three contribute to

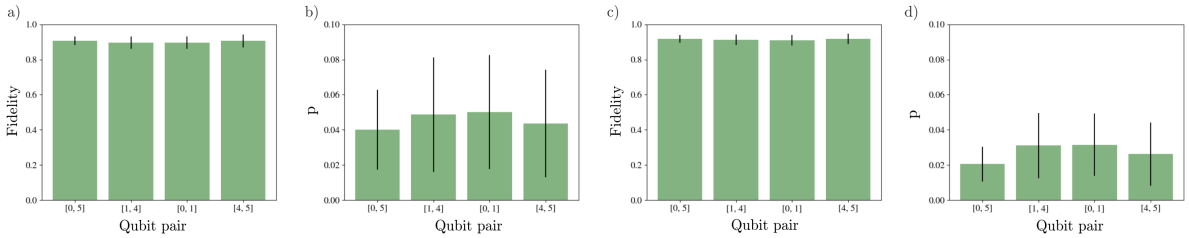

Figure 4. (a) Fidelity between experimental final state and model of final state with single-qubit depolarising noise applied. Results are shown separately for each of the four pairs generated using MQNC. Error bars indicate one standard deviation. (b) Value of the noise parameter p which maximises fidelity between model and experiment. (c), (d) The same plots for the model of single qubit depolarising noise applied before measurements.

the error in a final state, and a detailed error model meant to mimic an actual processor should ideally incorporate all of them. It turns out, however, that by studying only the gate error through a simple analytical model of depolarising noise, it is possible to gain a clear insight into a large portion of the noise within the protocol. Depolarising noise is given for a single qubit by the channel

$$\mathcal{E}(\rho) = p\frac{I}{2} + (1-p)\rho, \tag{1}$$

and models the worst case gate error where the state of the qubit is replaced by the maximally mixed state with probability p. That is to say, it models the scenario where there is some probability of all information in the state being lost to the environment. Single-qubit depolarising noise has two shortcomings as a general noise model in that it assumes noise to be symmetrical and not coherent, and as such it can only provide an approximation of a true noise channel. Nevertheless, it does account for some fraction of the total noise and allows us to study this fraction of the noise. In the case of many gates being applied to a single qubit it may happen (though it is not guaranteed) that biased noise cancels out and that the overall noise becomes approximately symmetrical. It was found that the single-qubit depolarising noise channel models noise in MQNC on `ibm_cairo` with high fidelity. This is likely due to readout error mitigation and the short circuit depth of MQNC lessening the effect of non-gate errors.

4.1. Noise acting on the final state

At first I modelled noise as single-qubit depolarising noise acting on the final 2-qubit graph states $|G_2\rangle = \frac{1}{\sqrt{2}}(|0+\rangle = |1-\rangle)$. The single-qubit depolarising noise channel acting on each qubit of the 2-qubit graph state yields the final state

$$\frac{1}{4}, \begin{pmatrix} 1 & (p-1)^2 & (p-1)^2 & -(p-1)^2 \\ (p-1)^2 & 1 & (p-1)^2 & -(p-1)^2 \\ (p-1)^2 & (p-1)^2 & 1 & -(p-1)^2 \\ -(p-1)^2 & -(p-1)^2 & -(p-1)^2 & 1 \end{pmatrix}.$$

in the case of equal depolarising noise on both qubits.

In Fig. 4 (a) the maximum fidelity between the experimental state and the ideal final state with equal amounts of depolarising noise applied to each qubit is shown for each pair of MQNC. By varying p and calculating the corresponding fidelity the value of p for which the fidelity is maximum can be determined. These are shown in Fig. 4 (b).

4.2. Noise applied prior to MQNC measurements

More insight into noise in MQNC on IBM processors can be gained by modelling noise applied before the final ZZ or XX measurements. I begin by initialising the density matrix of the

circuit to that of the state $|+\rangle^{\otimes 6}$. Controlled phase gates are then applied to produce the 6-qubit resource state for MQNC and then the single-qubit depolarising channel is applied to each qubit in turn after which measurements are made. The 2-qubit final states are obtained by means of the partial trace operation. The states take the form

$$\frac{1}{4}\begin{pmatrix} 1 & -1\,(p-1)^3 & -1\,(p-1)^3 & -1\,(p-1)^4 \\ -1\,(p-1)^3 & 1 & 1\,(p-1)^4 & 1\,(p-1)^3 \\ -1\,(p-1)^3 & 1\,(p-1)^4 & 1 & 1\,(p-1)^3 \\ -1\,(p-1)^4 & 1\,(p-1)^3 & 1\,(p-1)^3 & 1 \end{pmatrix}.$$

Using this model of the noise and repeating the previous analysis we obtain the results shown in Fig. 4 (c) and (d). While there is little difference in the fidelity between model and experiment compared to the case of noise applied to the final 2-qubit states, the noise parameter p is significantly less for the new model. This is a result of the final state density matrices of the new model containing $(1-p)^3$ and $(1-p)^4$ terms instead of the $(1-p)^2$ terms of the simple model. A greater value of p per qubit is required for noise applied after measurements to achieve the same fidelity between model and experiment as when the noise is applied prior to measurements. This leads to the physical interpretation that the amount of depolarising noise per qubit is greater in the final state than in the pre-measurement state, and hence the measurement has the effect of compounding the noise in the remaining qubits.

5. Conclusion

The purpose of this study was to investigate MQNC on superconducting technology which is available at this point in time. The main result was demonstrating that recent improvements in the hardware have made it possible to perform MQNC with final state fidelities upwards of 0.7 and as high as 0.9. Compared to the maximum cross-pair fidelity of 0.58 obtained just two years previously on the previous generation processor IBM Q 20 Tokyo, this represents a major improvement, and suggests that MQNC on superconducting hardware will likely become practical within the next few years. The improved results made it possible to study the noise experimentally in greater detail than before, and it was determined that the MQNC measurements have the effect of compounding single-qubit depolarising noise, so that the individual qubits in the final states have a higher amount of this noise than the individual qubits before measurement.

Acknowledgements

We thank Stellenbosch University, the Department for Science and Innovation (DSI) and the National Research Foundation (NRF) of South Africa. We also thank the University of Witwatersrand for access to the IBM processors via the ARUA network.

References

[1] Kimble H J 2008 *Nature* **453** 1023–1030
[2] Pompili M *et al.* 2021 *Science* **372** 259–264
[3] Chen Y A *et al.* 2021 *Nature* **589** 214–219
[4] Magnard P *et al.* 2020 *Phys. Rev. Lett.* **125**(26) 260502
[5] Mirhosseini M, Sipahigil A, Kalaee M and Painter O 2020 *Nature* **588** 599–603
[6] Hayashi M 2007 *Phys. Rev. A* **76**(4) 040301
[7] Kobayashi H, Le Gall F, Nishimura H and Rötteler M 2009 *Automata, Languages and Programming* ed Albers S, Marchetti-Spaccamela A, Matias Y, Nikoletseas S *et al.* (Berlin, Heidelberg: Springer Berlin Heidelberg) pp 622–633 ISBN 978-3-642-02927-1
[8] Matsuo T, Satoh T, Nagayama S and Van Meter R 2018 *Phys. Rev. A* **97**(6) 062328
[9] Pathumsoot P *et al.* 2020 *Phys. Rev. A* **101**(5) 052301
[10] Hein M, Eisert J and Briegel H J 2004 *Phys. Rev. A* **69**(6) 062311
[11] James D F, Kwiat P G, Munro W J and White A G 2005 *Asymptotic Theory of Quantum Statistical Inference: Selected Papers* (World Scientific) pp 509–538
[12] Georgopoulos K, Emary C and Zuliani P 2021 *Phys. Rev. A* **104** 062432